BMC Pediatrics

RESEARCH Open Access

Application of HRCT-based radiomics to predict interstitial lung disease for juvenile dermatomyositis

Lingke Liu[1,2†], Minfei Hu[1†], Yun Zhou[1], Fei Zheng[1], Xiaohui Ma[3], Li Yang[3], Yiping Xu[1], Liping Teng[1], Bin Hu[1], Meiping Lu[1] and Xuefeng Xu[1*]

Abstract

Background Interstitial lung disease (ILD) is a frequently observed pulmonary manifestation in juvenile dermatomyositis (JDM), and may significantly impact patient outcomes. Therefore, early lung involvement identification is essential. Radiomics is a new image analysis technique and might offer valuable information for the diagnosis of interstitial lung disease in juvenile dermatomyositis (JDM-ILD).

Methods We retrospectively analyzed clinical data of 56 children with JDM, and all participants gave written informed consent. These children were divided into the JDM group ($n=32$) and JDM-ILD group ($n=24$) based on chest high-resolution CT (HRCT). The lung intelligence kit (LK) software was used to outline the bilateral lung tissue structure automatically. The radiomics score combining with clinical variables was used to establish a prediction model for JDM-ILD.

Results A total of seven radiomics features including the maximum, mean, skewness, and kurtosis features for the First Order Features, the InverseVariance feature for the Gray Level Co-occurrence Matrix (GLCM) Features, the Size Zone NonUniformity Normalized feature for the Gray Level Size Zone Matrix(GLSZM)Features, and the Run Entropy feature for the Gray Level Run Length Matrix (GLRLM) Features were identified. The multivariable logistic regression revealed that anti-MDA5 antibody and radiomics score showed a significant correlation with the development of ILD in children with JDM. The combined prediction model based on radiomics score and anti-MDA5 antibody achieved good performance in predicting JDM-ILD in the training (0.92, 95% CI 0.82-1.00) and validation (0.93, 95% CI 0.83-1.00) groups.

Conclusion The nomogram combining radiomics and clinical variables achieved an optimal prediction of ILD in children with JDM. This approach may facilitate earlier detection of pulmonary involvement, support individualized risk stratification, and guide more proactive therapeutic interventions. Future studies should aim to validate this model in larger, prospective, and multicenter cohorts.

†Lingke Liu and Minfei Hu contributed equally to this work.

*Correspondence:
Xuefeng Xu
xuxuefeng@zju.edu.cn

Full list of author information is available at the end of the article

Highlights

- • Interstitial lung disease (ILD) is a severe complication of juvenile dermatomy-ositis (JDM).
- • Early lung involvement identification is essential for is essential for diagnosis and treatment of ILD.
- • Radiomics can offer valuable information for the diagnosis of interstitial lung disease in juvenile dermatomyositis.

Keywords High-resolution CT, Interstitial lung disease, Juvenile dermatomyositis, Nomogram, Radiomics

Introduction

Juvenile dermatomyositis (JDM) is a rare systemic autoimmune disease that manifests as symmetrical proximal muscle weakness, raised serum concentrations of muscle enzymes, characteristic skin rashes including heliotrope rash over the eyelids and Gottron's papules over the extensor joint surfaces [1]. JDM is also a systemic vascular lesion involving multiple organs such as the lungs, joints, heart and gastrointestinal tract [2]. Interstitial lung disease (ILD) is characterized by abnormal gas exchange, imaging and histopathological abnormalities, mainly involving alveoli and their surrounding tissues, interstitial lung, with dyspnea after activity as the primary manifestation, often secondary to various connective tissue diseases [3, 4]. ILD encompasses a group of disorders that affect the lung interstitium, leading to inflammation, fibrosis, and progressive lung damage. The severity of the disease can range from mild and stable to rapidly progressive forms that cause significant respiratory failure. ILD is a common pulmonary complication in adult myositis, with a prevalence between 30% and 50% and a high morbidity and mortality rate [5, 6]. More than one third of children with JDM have respiratory complications, and about 20% suffer from ILD [7]. JDM is also common etiology of connective tissue disease-related ILD [8]. Furthermore, rapidly progressive ILD is a major cause of mortality in JDM, resulting in a poor prognosis [9].

JDM-ILD may be asymptomatic in the early stage, symptoms such as cough and dyspnea may not be present until the disease has progressed. Furthermore, the lung parenchyma damage may be irreparable once the youngster exhibits respiratory symptoms. Therefore, early detection of lung involvement is crucial for the management and prognosis of children with JDM. Although chest high-resolution CT (HRCT) helps to determine the type of ILD and its distribution, assess the extent of the disease, and monitor its progression [10]. However, the insidious onset of JDM-ILD, the difficulty of early recognition and the difficulty of treatment are important factors that affect the prognosis of JDM [11]. Radiomics is a new image analysis technique that has been developed in recent years using an automated high-throughput extraction of large amounts of quantitative features of medical images, which can provide valuable information for the diagnosis, monitoring, and prognostic evaluation of diseases [12, 13]. The combination of the information of the lesion area and whole lung area would provide a more comprehensive information about JDM-ILD.

Therefore, the present study aimed to develop and validate an HRCT-based radiomics model, predicting the presence of ILD in children with JDM. A machine learning method was used to screen the characteristic parameters associated with the development of ILD.

Methods

Patients

The clinical and imaging data of children with JDM were collected from June 2014 to September 2021, at the Children's Hospital, Zhejiang University School of Medicine. HRCT is routinely performed as part of the initial evaluation for all children with JDM upon their first hospital admission, with the exception of those who have undergone a CT scan within the past three months. This is done to prevent missed diagnoses of ILD, particularly in cases with atypical symptoms. They were divided into a control group (JDM, $n = 32$) and an ILD group (JDM▪ILD, $n = 24$). The inclusion criteria are as follows: (a) relatively complete case data; (b) Age ≥ 5 years; (c) diagnosis of JDM met the classification criteria by EULAR/ACR 2017 [14]; (d) diagnosis of ILD was based on respiratory symptoms (cough and sputum or dyspnea), physical examination (velcro sounds), HRCT showing interstitial changes, and pulmonary function tests showing restrictive pulmonary ventilation dysfunction or pulmonary ventilation dysfunction. Additional diagnostic criteria included the presence of other clinical signs such as fever and fatigue, and a thorough evaluation of the patient's medical history. However, it is important to note that most patients were asymptomatic at the time of diagnosis. Furthermore, the HRCT patterns were closely examined for characteristic findings such as ground-glass opacities (GGO), reticular patterns, and interlobular septal thickening. Those JDM patients with incomplete case data, motion artifacts in HRCT images, and automatic segmentation failure of LK software were excluded (Fig. 1). This study was approved by the Ethics Review Board of Children's Hospital, Zhejiang University School of Medicine (2022-IRB-082). All procedures in this study were conducted in accordance with the Declaration of Helsinki. The clinical and imaging

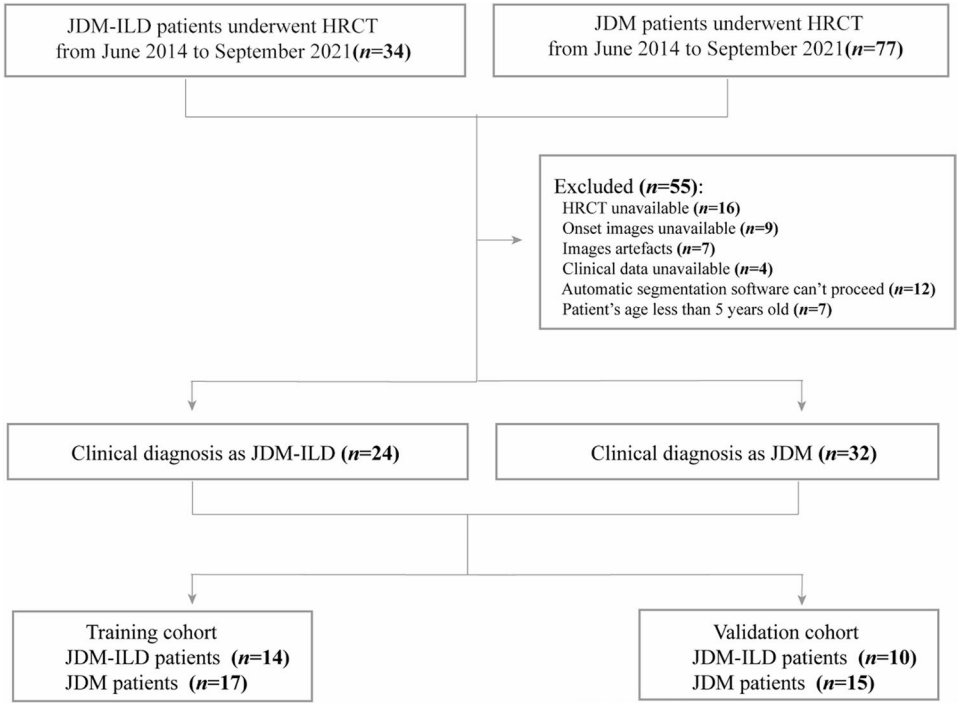

Fig. 1 The flowchart illustrates the steps for study recruitment and classification

data were also de-identified, and there was no additional risk to patients in this study.

HRCT Acquisition

All cases were scanned on a SIEMENS Emotion 16-row CT scanner, and HRCT was performed in all cases. There were no special requirements before the examination, and the scanning area was from the apical part of both lungs to 2 cm below the parallel line of the diaphragm angle of both ribs. Scanning conditions: 110–130 KV, automatic milliamp, the thoracic algorithm was used to thin and reorganize the layers, and the reorganized layer thickness and layer spacing were 0.8 mm.

HRCT Radiomics feature extraction

The LK software (Lung Intelligence Kit; GE Healthcare) was applied to segment the lung tissue of all HRCT images of children with JDM. The lung lobe segmentation algorithm in the LK software used the DenseVNet al.gorithm (Fig. 2) [15]. DenseVNet is a deep learning model specifically designed for medical image segmentation, which allows for more precise delineation of complex structures such as lung tissue in CT images. AK software (Artificial Intelligence Kit; GE Healthcare) was used to extract radiomics features from the segmented lung tissue, including First Order Features, Shape Features(2D,3D), GLCM features, GLSZM features, GLRLM Features, NGTDM features and GLDM features [16]. The radiomics features capture various texture, shape, and intensity variations that may not be apparent through standard imaging evaluation. The whole lung group data was used for feature screening.

Feature selection

The minor absolute shrinkage and selection operator LASSO regression machine learning model were built. This method avoids overfitting by L1 regularizing the sparse model. First, the data are standardized, then screened the features by two-sample t-test to exclude the variable elements with $P > 0.05$. Second, Spearman correlation analysis was used to evaluate the features' correlation; if the Spearman correlation coefficient was greater than 0.80, they would be considered to be redundant and excluded. Lastly, the total sample was randomly split, and 70% of the data was used for training and 30% for validation. Five-fold cross-validation in the training set cohort obtained a series of regularization parameters λ for the LASSO model. The best λ was selected to determine the feature selection and establish the radiomics score (Fig. 3) [17, 18]. The final radiomics score was calculated by combining the selected features, and it was used to predict the likelihood of ILD presence or progression in the cohort.

Evaluation of diagnostic performance

We used the selected radiomic characteristics to build the model to evaluate the diagnostic performance of the radiomic score. In addition, a new combining prediction model of radiomics score and clinical features was constructed to predict the development of ILD.

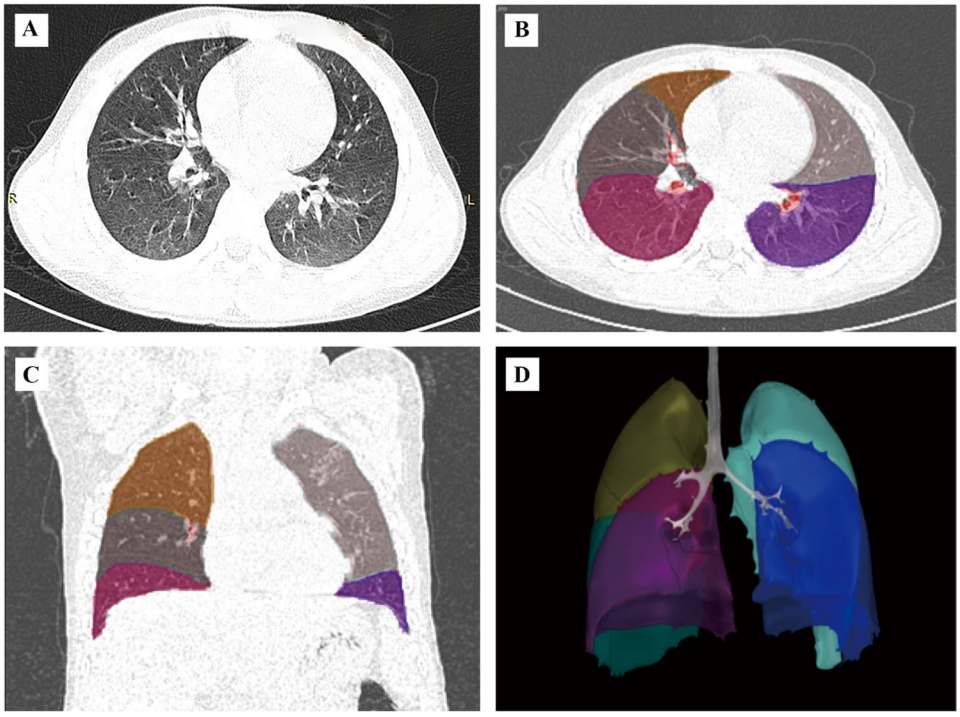

Fig. 2 HRCT imaging of JDM patients (**A**). Noted the illustration of the two lungs after segmentation by LK software based on cross-section (**B**), coronal plane (**C**), and three-dimensional (**D**) segmentation methods

Statistical analysis

Python 3.7 software was used to perform data downscaling and feature screening of radiological features and to construct radiomic scores [19]. R 4.0.5 software was for statistical analysis of clinical data with the two-sided test. The X^2 test was performed for categorical data, and the independent sample t-test was done for quantitative data conforming to normal distribution. The Mann-Whitney U test was used for non-normally distributed features. Univariable and multivariable logistic regression were for screening potential predictors. Feature selection, modeling, and internal validation were also implemented in R software, and Nomogram plots were drawn using the RMS package [18]. A $P < 0.05$ was considered to be statistically significant.

Result

Clinical characteristics of children with JDM

Fifty-six of patients with JDM were included in this study and randomly divided into the training cohort ($n = 31$, 55%) and an external validation cohort ($n = 25$, 45%). Among the children, the mean age was 8.9 ± 2.9; 24 (43%) were boys, and 32 (57%) were girls. Clinical data from the training and validation groups did not differ significantly. A detailed comparison of clinical characteristics between JDM with ILD (JDM-ILD) and without ILD (control) groups is shown in Table 1. The imaging patterns of HRCT in JDM-ILD mainly included ground glass opacity (GGO, 66.7%), reticular & linear opacities (54.2%), interlobular septal thickening (50.0%), pleural thickening (45.8%), nodular opacities (37.5%) and bronchial wall thickening (29.2%).

Construction of radiomics score based on radiomics feature selection

We extracted 1316 radiomic features from each patient's medical images, and a two-sample t-test analyzed 377 segments to show significant differences between the JDM and JDM-ILD groups. Subsequently, 50 features were screened out by Spearman correlation. The remaining features were screened by the LASSO regression algorithm, and finally a total of 7 radiomics features including the maximum, mean, skewness, and kurtosis features for the First Order Features, the InverseVariance feature for the GLCM Features, the Size Zone NonUniformity Normalized feature for the GLSZM Features, and the Run Entropy feature for the GLRLM features were obtained (Fig. 3). The univariate logistic regression analysis demonstrated that these seven radionics features can independently predict the development of ILD in children with JDM. Furthermore, the radiomics score integrating these seven features has the greatest predictive effect on JDM-ILD (Table 2).

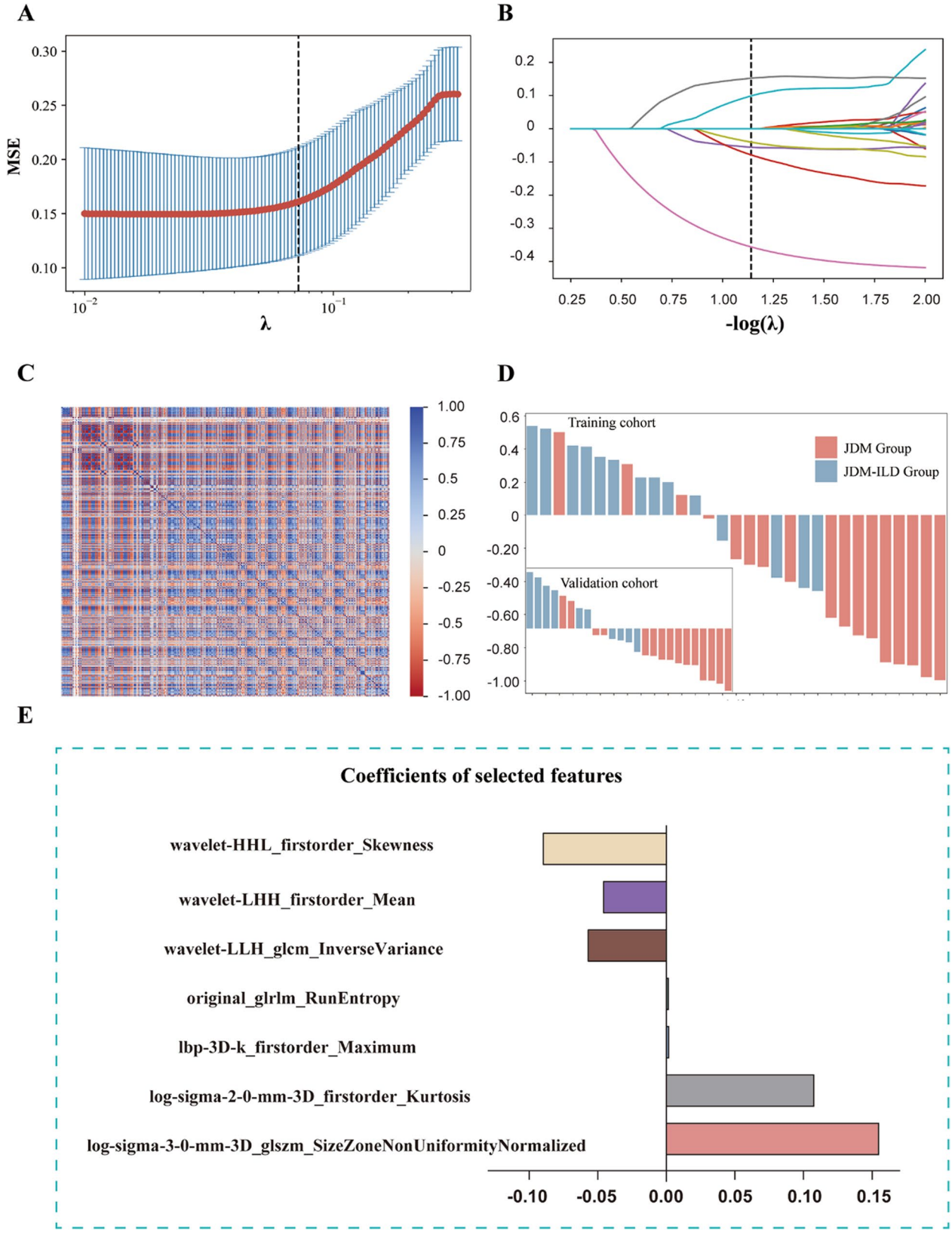

Fig. 3 (See legend on next page.)

(See figure on previous page.)

Fig. 3 Radiomics feature selection and radiomics histology score validation. **A** The selection of the tuning parameter (lambda) in the LASSO model using five-fold cross-validation with a minimum criterion. **B** Color lines show the coefficients of the features. The dashed vertical lines of (**A**, **B**) determine the best values, and seven features with coefficients that are not zero are selected to construct the radiomics score. **C** The covariance matrix of radiomics features before correlation filtering. **D** Training and validation of the established radiomics score for each patient in the cohort. **E** Coefficients of the selected radiomics features extracted from MRI

Clinical predictors of JDM-ILD in children

Univariate logistic regression analysis showed significant correlations between the children's age (OR, 1.017; 95% CI 1.001 to 1.034), arthralgia (OR, 4.2; 95% CI 1.162 to 17.702), anti-MDA5 (melanoma differentiation-associated gene 5) antibody (OR, 22.142; 95% CI 3.717 to 426.916), radiomics features, and radiomics score, and the development of ILD (Table 2). There were no statistically significant associations between other clinical characteristics and the development of ILD ($P > 0.05$, Table 2). However, the multivariate logistic regression revealed that only anti-MDA5 antibody (OR, 36.79; 95% CI 4.19 to 202106.5, $P < 0.01$) and radiomics score (OR, 1340.59; 95% CI 33.41 to 15787.05, $P < 0.01$) showed significant correlations with the development of ILD, further suggesting that anti-MDA5 antibody played an important role in the development of ILD among children with JDM (Fig. 4A).

Discriminating nomogram development and validation

A nomogram based on radiomic score and anti-MDA5 antibody exhibited significant differences in predicting JDM-ILD (Fig. 4). In both training and validation cohorts, the nomogram was highly discriminative in predicting JDM-ILD, with an AUC of 0.92 (95% CI, 0.83-1.00) for the training cohort and 0.93 (95% CI, 0.83-1.00) for the validation cohort. In contrast, bootstrap resampling showed good agreement in predicting JDM-ILD in both training and validation cohorts (Fig. 4). In addition, combining radiomic score with anti-MDA5 antibody significantly improved performance among all the patients (AUC 0.85; 95% CI 0.75–0.95, sensitivity and specificity of 83.3% and 75.0% vs. AUC 0.92; 95% CI 0.85-98, sensitivity and specificity of 87.5% and 81.2%; $n = 56$, $P = 0.04$) (Fig. 4).

Role of radiomics in predicting JDM-ILD

In the present study, we identified a notable finding: ten JDM-ILD children developed ILD during follow-up that had been undetected by radiologists at initial diagnosis. Of particular interest, five of these cases demonstrated relatively elevated radiomic scores (ranging from 0.56 to 0.65), implying that radiomic analysis may possess the capability to discern subtle pathological alterations potentially overlooked in conventional radiological assessment (Table 3). The radiomic score, derived from HRCT imaging, serves as a quantitative predictor for ILD likelihood in JDM patients. This predictive model demonstrates a spectrum of risk stratification, where higher scores (e.g., patient 1: 0.61) indicate increased ILD probability, while lower scores (e.g., patient 9: 0.27) suggest reduced risk, though they do not completely exclude the possibility of disease presence.

Nevertheless, it is imperative to recognize the potential limitations of this predictive model. False positive results may arise from imaging artifacts or confounding pulmonary conditions, whereas false negatives could occur in early-stage ILD where radiological manifestations remain subtle. The radiomic score was established through linear regression analysis, with the optimal threshold determined by maximizing the combined sensitivity and specificity, as evidenced by the receiver operating characteristic (ROC) curve analysis.

Discussion

ILD is the most common complication of JDM with a high mortality rate, which seriously affects the quality of life and prognosis of patients [20]. The development of ILD might be involved in genetics, environment, and immune mechanism [21]. The previous study demonstrated that the prevalence of ILD in PM/DM (Polymyositis/Dermatomyositis) was 50% in Asia, 23% in America, and 26% in Europe, highlighting potential genetic and environmental differences in the pathogenesis of ILD [22]. Although the incidence of ILD in JDM patients is significantly lower than that in adults with PM/DM [7, 22]; early and timely diagnosis of JDM-ILD would contribute to better controlling the JDM and improving its prognosis.

The chest HRCT patterns in patients with JDM-ILD mainly manifested as GGO, reticulation, traction bronchiectasis, and consolidation [23]. Our study showed similar HRCT patterns in patients with JDM-ILD, including GGO, interlobular septal thickening, pleural thickening, and nodular opacities. Differences in radiomic scores have been observed between various radiographic patterns in ILD. For example, studies have shown that patterns such as GGO and reticulation exhibit distinct radiomic features [24]. In particular, GGO has been associated with early-stage disease and might reflect subtle changes in the lung parenchyma, which are often missed by visual inspection [25]. Reticulation, on the other hand, is typically seen in more advanced stages of ILD and may have different radiomic characteristics. Radiomic features extracted from HRCT images can provide valuable insights into disease progression and help distinguish

Table 1 Association of patient characteristics in the training and validation cohorts

Characteristic	Training Cohort, No. (%)			Validation Cohort, No. (%)		
	JDM-ILD (*n* = 14)	Control (*n* = 17)	*P* value	JDM-ILD (*n* = 10)	Control (*n* = 15)	*P* value
Age, mean ± SD, y	9.1 ± 2.5	8.3 ± 3.2	0.42	10.9 ± 2.9	8.1 ± 2.6	0.02 *
Sex			1.00			0.69
Male	7 (50.0)	8 (47.0)		3 (30.0)	6 (40.0)	
Female	7 (50.0)	9 (53.0)		7 (70.0)	9 (60.0)	
Weight, mean ± SD, kg	32.2 ± 15.1	27.0 ± 8.6	0.26	32.1 ± 11.6	25.8 ± 7.4	0.11
Fever	4 (28.6)	2 (11.8)	0.37	3 (30.0)	1 (6.7)	0.27
Arthrodynia	5 (35.7)	2 (11.8)	0.20	3 (30.0)	3 (20.0)	0.65
Muscle strength (CMAS), Mean ± SD[1]	7.7 ± 1.6	7.8 ± 1.5	0.77	8.3 ± 1.4	8.2 ± 0.9	0.83
WBC						
Median (IQR),/uL	6.8 ± 2.2	7.2 ± 2.2	0.62	5.5 ± 1.5	5.9 ± 1.4	0.46
Outside reference range	1 (7.1)	2 (11.7)	1.00	1 (10.0)	2 (13.3)	1.00
ESR						
Median (IQR), mm/h	20.5 (9.0–29.5)	8.0 (7.0–22.0)	0.14	17 (9.0–37.3)	13 (8.0–26.0)	0.47
Outside reference range	7 (50.0)	4 (23.5)	0.15	5 (50.0)	6 (40.0)	0.69
CRP						
Median (IQR), mg/L	1.2 (0.5–4.7)	1.0 (0.5–2.5)	0.63	0.7 (0.5–3.2)	1.4 (1.0–3.0)	0.41
Outside reference range	3 (21.4)	1 (5.9)	0.30	1 (10.0)	1 (6.7)	1.00
CK						
Median (IQR), U/L	233 (97-1671)	336 (139–2795)	0.63	1377 (184–5559(	318 (128–837)	0.22
Outside reference range	13 (92.9)	16 (94.1)	1.00	10 (100.0)	14 (93.3)	1.00
CK_MB						
Median (IQR), U/L	32 (23.2–65)	38 (23.5–85)	0.77	64 (27.2-166.7)	39 (28–69)	0.29
Outside reference range	13 (92.9)	16 (94.1)	1.00	10 (100.0)	14 (93.3)	1.00
LDH						
Median (IQR), U/L	772.5 (499.7-977.2)	132 (100-243.5)	0.89	86.5 (62-264.2)	79 (38–132)	0.26
Outside reference range	14 (100)	17 (100)	1.00	10 (100.0)	14 (93.3)	1.00
ALT						
Median (IQR), U/L	53.5 (27-120.5)	78 (56–116)	0.47	66 (24.2–78.7)	45 (17–65)	0.27
Outside reference range	8 (57.0)	14 (82.0)	0.23	6 (60.0)	8 (53.3)	1.00
AST						
Median (IQR), U/L	137.5 (48.7-242.7)	132 (100-243.5)	0.89	86.5 (62-264.2)	79 (38–132)	0.26
Outside reference range	9 (64.3)	13 (76.5)	0.69	7 (70.0)	9 (60.0)	0.69
Anti-MDA5, Positive[2]	5 (35.7)	0 (0)	0.01*	5 (50)	1 (6.6)	0.02*
Anti-NXP2, Positive[2]	3 (21.4)	1 (5.9)	0.30	2 (20.0)	1 (6.7)	0.54
Anti_Ro52, Positive[2]	1 (7.1)	1 (5.9)	1.00	5 (50%)	2 (13.3)	0.08
Anti-PL_7, Positive[2]	0 (0)	0 (0)	1.00	1 (10)	0 (0)	0.40
Anti-PL_12, Positive[2]	1 (7.1)	0 (0)	0.45	0 (0)	0 (0)	1.00
ANA, Positive	5 (35.7)	3 (17.6)	0.41	3 (30.0)	1 (6.7)	0.27

Abbreviations: *JDM* Juvenile dermatomyositis, *WBC* White blood cell, *ESR* Erythrocyte sedimentation rate, *CRP* C-reactive protein, *CK* Creatine kinase, *CK_MB* Creatine kinase isoenzyme-MB, *LDH* Lactic dehydrogenase, *ALT* Alanine aminotransferase, *AST* Aspartate aminotransferase, *ANA* Anti-nuclear immune body, *SI* Conversions, WBC to $\times 10^9$ per liter

[1]muscle strength is measured by CMAS, and partial missing data were imputed by regression imputation according to the muscle strength

[2]patients who did not undergo the myositis-specific autoantibodies (MSAs) and myositis-associated autoantibodies (MAAs) were regarded as negative

*$P < 0.05$, in statistical analyses

between different ILD subtypes [26]. Adult dermatomyositis-associated ILD are much more likely to present with consolidations and rapidly progressive ILD [27]. In general, the common HRCT patterns for ILD in anti-MDA5 positive patients were nonspecific interstitial pneumonia [28]. In contrast, children with JDM-ILD present frequently with GGO on HRCT, possibly suggesting that children could have a better response to treatment and a better prognosis.

There is increasing evidence that myositis-specific autoantibodies (MSA) play a major role in management of idiopathic inflammatory myopathies-associated ILD. Anti-MDA5 and anti-aminoacyl tRNA synthetase (ARS, e.g. PL-7, PL-12) positive patients had higher rates of

Table 2 Predictors for the development of ILD in JDM

Variable	OR	CI (2.50-97.5%)	*P* value
weight	1.05	1.00-1.12	0.06
Age (month)	1.02	1.00-1.03	0.04*
Sex	0.92	0.31–2.68	0.88
Fever	3.982	0.97–8.44	0.07
Arthralgia	4.2	1.16–17.70	0.04*
Muscle strength (CMAS)	0.962	0.65–1.42	0.85
Rash	1.4	0.37–5.98	0.63
C reactive protein (CRP)	1.032	0.97–1.17	0.38
Erythrocyte sedimentation rate (ESR)	1.02	0.98–1.06	0.35
Creatine kinase (CK)	1.00	0.99-1.00	0.25
Lactate dehydrogenase (LDH)	1.00	1.00–1.00	0.07
Alanine aminotransferase (ALT)	0.99	0.98–1.01	0.95
Aspartate aminotransferase (AST)	1.00	0.99–1.01	0.24
Anti-MDA5	22.14	3.72-426.92	< 0.01**
Anti-Ro52	3.95	0.77–29.55	0.12
Anti-NXP2	3.95	0.77–29.55	0.12
Antinuclear antibody (ANA)	3.5	0.95–14.88	0.07
lbp_3D_k_firstorder_Maximum	2.12	1.18–4.16	0.02*
log_sigma_2_0_mm_3D_firstorder_Kurtosis	3.75	1.77–9.89	< 0.01**
log_sigma_3_0_mm_3D_glszm_SizeZoneNonUniformityNormalized	7.14	2.73–26.45	< 0.01**
original_glrlm_RunEntropy	2.62	1.40–5.61	< 0.01 **
wavelet_LLH_glcm_InverseVariance	0.37	0.17–0.70	< 0.01 **
wavelet_LHH_firstorder_Mean	0.43	0.22–0.77	< 0.01**
wavelet_HHL_firstorder_Skewness	465.84	27.72-15787.05	< 0.001 **
Radiomics score	2,398,321	4123.05-58813150000.00	< 0.001 ***

ILD, whereas anti-transcription intermediary factor 1-gamma (anti-TIF1γ), anti-Mi-2 and anti-nuclear matrix protein 2 (anti-NXP-2) antibodies were associated with a decreased risk of ILD [28, 29]. Anti-MDA5 autoantibody could be useful not only for a disease marker of ILD associated with JDM, but also as a predictive marker for the complication of ILD [30, 31]. Anti-MDA5 is distinguished from anti-synthetase autoantibody-positive dermatomyositis by less frequent ILD and lower CK levels [32]. Consistent with the previous studies, we also found a significant association between positive MDA5 antibody and JDM▪ILD. However, we failed to perform further analysis for other MSA due to the small number of cases. Additionally, clinical symptoms such as hyperthermia and arthralgia could be associated with the development of ILD [23]. In our study, although multivariable logistic regression analysis did not find a significant predictor in clinical variables, univariable regression analysis suggested arthralgia as a predictor for ILD. These results further revealed laboratory test and clinical manifestations could be used to predict the development of ILD in children with JDM.

Recently, disease prediction models of radiomics based on chest HRCT have increasingly been reported, including predicting residual lung lesions in COVID-19 patients after hospital discharge, survival in critically ill COVID-19 patients, and the mortality of patients with rheumatoid arthritis-associated ILD [33–35]. Notably, a study by *Sato* et al. demonstrated that the combination of anti-MDA5 antibodies and chest CT imaging could predict the development of ILD in JDM [23]. In the present study, we quantitatively analyzed chest HRCT data through extracting radiomics features, further exploring the information of radiomics. To our knowledge, this is the first report on the prediction of the development of ILD in JDM patients using chest HRCT radiomics.

In our institution, the standard treatment for JDM-ILD typically involves a combination of immunosuppressive agents, such as corticosteroids plus Mycophenolate Mofetil or Tacrolimus, aimed at reducing inflammation and controlling disease progression. In cases of severe or refractory disease, biologic agents like JAK inhibitors or rituximab may be considered. Early initiation of treatment is critical to improve outcomes, especially in patients with rapidly progressive ILD.

With regard to radiomics, the selection of images and radiomic features appears to be essential. However, many radiomics features are redundant due to different CT scanners and acquisition parameters [36]. So far, there is still no consensus on the degree of radiomics reliability that has been achieved in radiomics research [37]. In this study, we selected chest phase CT images and evaluated characteristics for correlation to minimize the inherent defects of CT radiomics features. The radiomics score integrating seven radiomic features was used to build radiomics prediction model and distinguish JDM-ILD from children with JDM. Furthermore, combining radiomic score with MDA5 antibody significantly improved the predicted performance of the model. JDM children with a score of 104 or more could have a high-risk of ILD. For example, a JDM children with positive anti-MDA5 antibody (49 points) plus radiomics score (55 points) would have a total of 104 points, strongly indicating the development of ILD. Significantly, our study also included a detailed analysis of baseline characteristics and radiomic scores in a cohort of ten children with JDM-ILD. Intriguingly, while none of these patients had a clinical diagnosis of ILD at their initial evaluation, longitudinal follow-up revealed that five cases with elevated radiomic scores subsequently developed ILD. This critical observation strongly suggests that radiomic analysis may serve as a highly sensitive diagnostic tool, capable

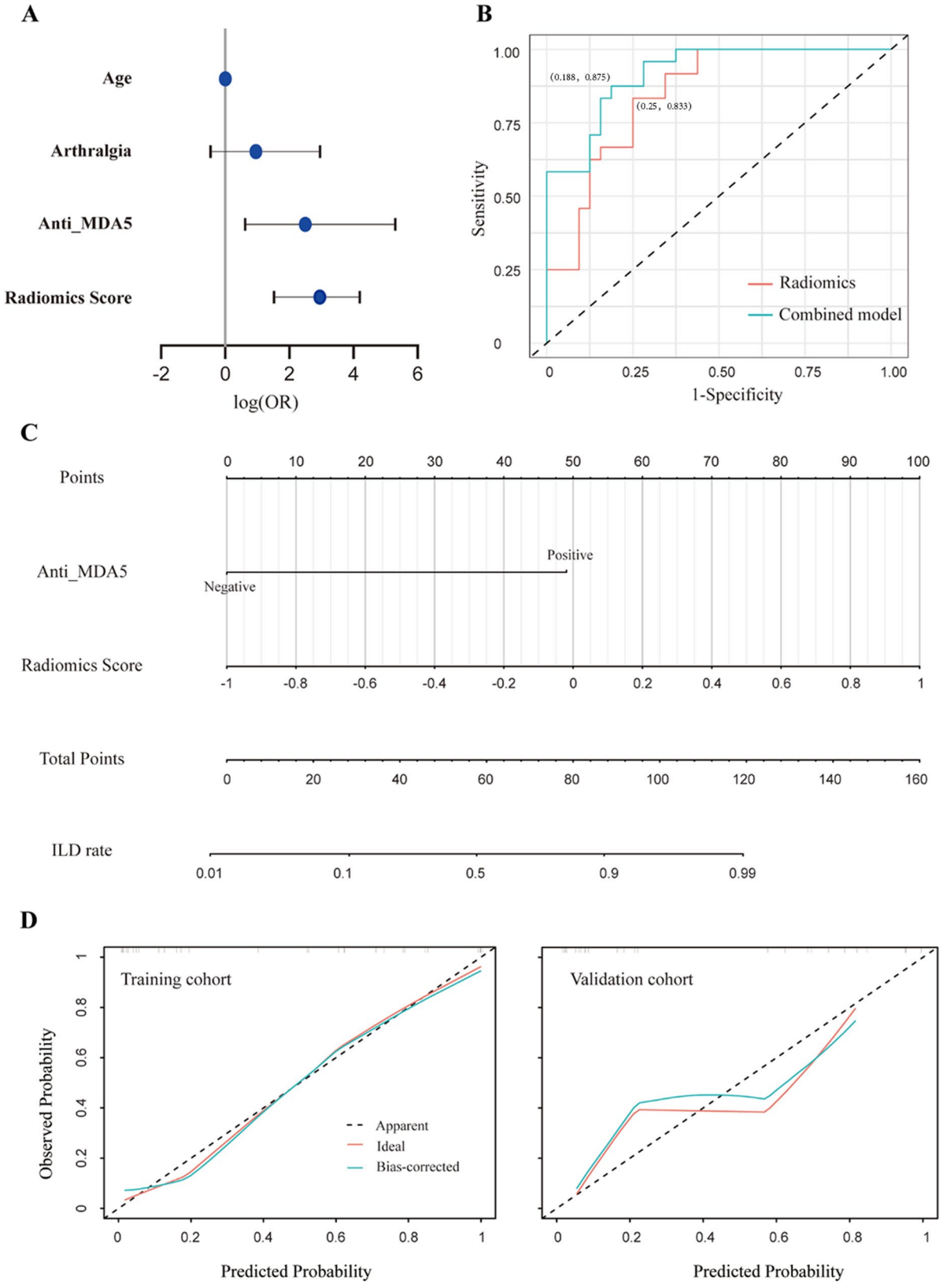

Fig. 4 The analysis of relevant characteristics and the construction of a radiomics nomogram. **A** Logarithm of the Odds ratio (OR) for the independent risk factors. **B** Discriminant and combined model of radiomics. Receiver operating characteristic (ROC) curves for linear discriminant analysis of radiomics scores and clinical features combined with radiomics features in all patients. **C** The nomogram combined associated clinical factors and radiomics score to estimate the risk of suffering JDM-ILD. **D** The bootstrapped estimates of calibration accuracy for the nomogram at the training and validation cohorts

Table 3 Baseline characteristics and radiomic scores of JDM patients

Patient ID	Age (years)	Sex	Anti-MDA5 Antibody (Positive/Negative)	CRP (mg/L)	ESR (mm/h)	Radiomic Score
1	6.3	Female	Positive	0.5	44	0.61
2	9.4	Female	Negative	3	35	0.64
3	14	Female	Negative	0.5	45	0.65
4	14.4	Male	Positive	1.8	28	0.61
5	13.3	Male	Negative	0.5	6	0.56
6	6.5	Male	Negative	0.5	9	0.32
7	13	Male	Positive	0.5	13	0.39
8	12.1	Female	Positive	1	21	0.28
9	10.6	Male	Negative	6.8	1	0.27
10	6.1	Male	Negative	1	33	0.31

of identifying subclinical pulmonary alterations that may escape detection through conventional radiological assessment.

There are several limitations to this study that should be acknowledged. First, due to the rarity of juvenile dermatomyositis (JDM), the sample size was relatively small, which may reduce the statistical power and limit the generalizability of the findings. Although internal validation was performed, future studies with larger sample sizes and external validation cohorts are needed to improve the robustness and applicability of the model. Second, this was a retrospective study, and thus lacked the prospective control necessary to establish temporality or minimize selection bias. Additionally, the ability to obtain stable radiomic features may have been influenced by variability in image acquisition; however, previous studies have reported that the impact of segmentation-related variability on radiomic reproducibility is relatively minor [37]. In our study, the use of fully automated segmentation through the LK software also helped to mitigate such concerns. Third, children's age plays a crucial role in HRCT image quality—especially in younger children who may have difficulty cooperating during breath-holding, leading to suboptimal lung inflation. Therefore, only children aged five years or older were included in this analysis. As a result, the proposed radiomics model may not be applicable to younger pediatric patients. Finally, while anti-MDA5 was identified as a significant clinical predictor, the relatively low frequency of other myositis-specific autoantibodies (MSAs) limited our ability to evaluate their contribution to interstitial lung disease (ILD) development.

Conclusions

The present study combined radiomics features based on chest HRCT and clinical variable and developed a nomogram to predict the development of ILD in children with JDM. The developed discriminative model based on radiomics would contribute to making better clinical evaluation and guiding early therapeutic decisions.

Abbreviations

ILD	Interstitial lung disease
JDM	Juvenile dermatomyositis
JDM-ILD	Interstitial lung disease in juvenile dermatomyositis
HRCT	High-resolution CT
LK	The lung intelligence kit
GLCM	Gray Level Co-occurrence Matrix
GLSZM	Gray Level Size Zone Matrix
GLRLM	Gray Level Run Length Matrix
GGO	Ground glass opacity
anti-MDA5	Melanoma differentiation-associated gene5
PM/DM	Polymyositis/Dermatomyositis
MSA	Myositis-specific autoantibodies
ARS	Anti-aminoacyl tRNA synthetase
anti-TIF1γ	Anti-transcription intermediary factor 1-gamma
anti-NXP-2	Anti-nuclear matrix protein 2

Acknowledgements
Not applicable.

Statement
While the program has not yet been made publicly available, we are exploring options to share the code and model with the broader research community for validation purposes.

Authors' contributions
L and X wrote the main manuscript text. H prepared all the figures. All authors collected data and reviewed the manuscript.

Funding
This work was supported by fund from the National Natural Science Foundation of China (81871220).

Data availability
The datasets used and/or analysed during the current study available from the corresponding author on reasonable request.

Ethics approval and consent to participate
This study was approved by the Ethic Review Board of Children's Hospital, Zhejiang University School of Medicine. (2022-IRB-082). All procedures in this study were conducted in accordance with the Declaration of Helsinki. Written Informed consent was obtained from all the parents/Guardians of the participating children.

Consent for publication
Not applicable.

Competing interests
The authors declare no competing interests.

Author details
[1]Department of Rheumatology Immunology & Allergy, The Children's Hospital, National Clinical Research Center for Child Health, Zhejiang University School of Medicine, Binsheng Rd 3333, Binjiang District, Hangzhou 310052, P.R. China

[2]Department of Pediatrics, The Affiliated Hospital of Shaoxing University, Shaoxing 312000, PR China
[3]Medical Imaging, The Children's Hospital, Zhejiang University School of Medicine, National Clinical Research Center for Child Health, Hangzhou 310052, PR China

Received: 15 May 2024 / Accepted: 16 July 2025
Published online: 02 August 2025

References

1. Feldman BM, Rider LG, Reed AM, Pachman LM. Juvenile dermatomyositis and other idiopathic inflammatory myopathies of childhood. Lancet. 2008;371(9631):2201–12.
2. Hussain A, Rawat A, Jindal AK, Gupta A, Singh S. Autoantibodies in children with juvenile dermatomyositis: a single centre experience from North-West India. Rheumatol Int. 2017;37(5):807–12.
3. Ramamurthy MB, Goh DY, Lim MT. Rare lung diseases: interstitial lung diseases and lung manifestations of rheumatological diseases. Indian J Pediatr. 2015;82(10):956–61.
4. Cerro Chiang G, Parimon T. Understanding interstitial lung diseases associated with connective tissue disease (CTD-ILD): genetics, cellular pathophysiology, and biologic drivers. Int J Mol Sci. 2023;24(3):2405. https://doi.org/10.3390/ijms24032405
5. Richardson AE, Warrier K, Vyas H. Respiratory complications of the rheumatological diseases in childhood. Arch Dis Child. 2016;101(8):752–8.
6. Rai M, Parthasarathi A, Beeraka NM, Kaleem Ullah M, Malamardi S, Padukudru S, Siddaiah JB, Uthaiah CA, Vishwanath P, Chaya SK, et al. Circulatory serum Krebs von den lungen-6 and surfactant protein-D concentrations predict interstitial lung disease progression and mortality. Cells. 2023;12(9):1281. https://doi.org/10.3390/cells12091281
7. Robinson AB, Reed AM. Clinical features, pathogenesis and treatment of juvenile and adult dermatomyositis. Nat Rev Rheumatol. 2011;7(11):664–75.
8. Xu X, Liu L, Xu X, Ma Q, Teng L, Zhou H, Yang L, Lu M. Etiologic profile of older children with diffuse radiological changes in eastern China. Front Pediatr. 2022;10:823350.
9. Yesilbas O, Yildiz M, Yozgat CY, Tahaoglu I, Yazan H, Cakir E, Adrovic A, Sahin S, Barut K, Kasapcopur O. A fatal interstitial lung disease in an anti-MDA5 antibody negative patient with juvenile dermatomyositis. Turk J Pediatr. 2021;63(5):903–8.
10. García-Peña P, Boixadera H, Barber I, Toran N, Lucaya J, Enríquez G. Thoracic findings of systemic diseases at high-resolution CT in children. Radiographics. 2011;31(2):465–82.
11. Kobayashi N, Takezaki S, Kobayashi I, Iwata N, Mori M, Nagai K, Nakano N, Miyoshi M, Kinjo N, Murata T, et al. Clinical and laboratory features of fatal rapidly progressive interstitial lung disease associated with juvenile dermatomyositis. Rheumatology (Oxford). 2015;54(5):784–91.
12. Lambin P, Rios-Velazquez E, Leijenaar R, Carvalho S, van Stiphout RG, Granton P, Zegers CM, Gillies R, Boellard R, Dekker A, et al. Radiomics: extracting more information from medical images using advanced feature analysis. Eur J Cancer. 2012;48(4):441–6.
13. Shi L, Yang M, Yao J, Ni H, Shao H, Feng W, He Z, Ni B. Application of computed tomography-based radiomics combined with clinical factors in the diagnosis of malignant degree of lung adenocarcinoma. J Thorac Disease. 2022;14(11):4435–48.
14. Lundberg IE, Tjärnlund A, Bottai M, Werth VP, Pilkington C, Visser M, Alfredsson L, Amato AA, Barohn RJ, Liang MH, et al. 2017 European league against rheumatism/American college of rheumatology classification criteria for adult and juvenile idiopathic inflammatory myopathies and their major subgroups. Ann Rheum Dis. 2017;76(12):1955–64.
15. Xing H, Zhang X, Nie Y, Wang S, Wang T, Jing H, Li F. A deep learning-based post-processing method for automated pulmonary lobe and airway trees segmentation using chest CT images in PET/CT. Quant Imaging Med Surg. 2022;12(10):4747–57.
16. Qiao J, Zhang X, Du M, Wang P, Xin J. (18)F-FDG PET/CT radiomics nomogram for predicting occult lymph node metastasis of non-small cell lung cancer. Front Oncol. 2022;12: 974934.
17. Tibshirani R. Regression shrinkage and selection via the Lasso. J Roy Stat Soc: Ser B (Methodol). 1996;58(1):267–88.
18. Hu M, Zheng F, Ma X, Liu L, Shen C, Wu J, Wang C, Yang L, Xu Y, Zou L et al. Assessment of Thigh MRI Radiomics and Clinical Characteristics for Assisting in Discrimination of Juvenile Dermatomyositis. *J Clin Med* 2022, 11(22).
19. van Griethuysen JJM, Fedorov A, Parmar C, Hosny A, Aucoin N, Narayan V, Beets-Tan RGH, Fillion-Robin JC, Pieper S, Aerts H. Computational radiomics system to Decode the radiographic phenotype. Cancer Res. 2017;77(21):e104–7.
20. DeWane ME, Waldman R, Lu J. Dermatomyositis: clinical features and pathogenesis. J Am Acad Dermatol. 2020;82(2):267–81.
21. Montesi SB, Fisher JH, Martinez FJ, Selman M, Pardo A, Johannson KA. Update in interstitial lung disease 2019. Am J Respir Crit Care Med. 2020;202(4):500–7.
22. Sun KY, Fan Y, Wang YX, Zhong YJ, Wang GF. Prevalence of interstitial lung disease in polymyositis and dermatomyositis: a meta-analysis from 2000 to 2020. Semin Arthritis Rheum. 2021;51(1):175–91.
23. Sato S, Uejima Y, Nanbu M, Suganuma E, Takano T, Tanaka R, Kabuki T, Oguma E, Oh-Ishi T, Kawano Y. Clinical analysis and outcome of interstitial lung disease complicated with juvenile dermatomyositis and juvenile polymyositis. Mod Rheumatol. 2017;27(4):652–6.
24. Yang CC, Chen CY, Kuo YT, Ko CC, Wu WJ, Liang CH, Yun CH, Huang WM. Radiomics for the prediction of response to antifibrotic treatment in patients with idiopathic pulmonary fibrosis: a pilot study. Diagnostics. 2022;12(4):1002. https://doi.org/10.3390/diagnostics12041002.
25. Shin B, Oh YJ, Kim J, Park SG, Lee KS, Lee HY. Correlation between CT-based phenotypes and serum biomarker in interstitial lung diseases. BMC Pulm Med. 2024;24(1):523.
26. Frix AN, Cousin F, Refaee T, Bottari F, Vaidyanathan A, Desir C, Vos W, Walsh S, Occhipinti M, Lovinfosse P, et al. Radiomics in lung diseases imaging: state-of-the-art for clinicians. J Pers Med. 2021;11(7):602. https://doi.org/10.3390/jpm11070602
27. Long K, Danoff SK. Interstitial lung disease in polymyositis and dermatomyositis. Clin Chest Med. 2019;40(3):561–72.
28. Teel A, Lu J, Park J, Singh N, Basharat P. The role of Myositis-Specific autoantibodies and the management of interstitial lung disease in idiopathic inflammatory myopathies: a systematic review. Semin Arthritis Rheum. 2022;57:152088.
29. Vega P, Ibarra M, Prestridge A, Pachman LM. Autoantibody to PL-12 (anti-alanyl-tRNA synthetase) in an African American girl with juvenile dermatomyositis and resolution of interstitial lung disease. J Rheumatol. 2011;38(2):394–5.
30. Tansley SL, Betteridge ZE, Gunawardena H, Jacques TS, Owens CM, Pilkington C, Arnold K, Yasin S, Moraitis E, Wedderburn LR, et al. Anti-MDA5 autoantibodies in juvenile dermatomyositis identify a distinct clinical phenotype: a prospective cohort study. Arthritis Res Ther. 2014;16(4):R138.
31. Kobayashi I, Okura Y, Yamada M, Kawamura N, Kuwana M, Ariga T. Anti-melanoma differentiation-associated gene 5 antibody is a diagnostic and predictive marker for interstitial lung diseases associated with juvenile dermatomyositis. J Pediatr. 2011;158(4):675–7.
32. Mamyrova G, Kishi T, Shi M, Targoff IN, Huber AM, Curiel RV, Miller FW, Rider LG. Anti-MDA5 autoantibodies associated with juvenile dermatomyositis constitute a distinct phenotype in North America. Rheumatology. 2021;60(4):1839–49.
33. Huang J, Wu F, Chen L, Yu J, Sun W, Nie Z, Liu H, Yang F, Zheng C. CT-based radiomics helps to predict residual lung lesions in COVID-19 patients at three months after discharge. Diagnostics. 2021;11(10):1814. https://doi.org/10.3390/diagnostics11101814.
34. Xiao F, Sun R, Sun W, Xu D, Lan L, Li H, Liu H, Xu H. Radiomics analysis of chest CT to predict the overall survival for the severe patients of COVID-19 pneumonia. Phys Med Biol. 2021;66(10):105008. https://doi.org/10.1088/1361-6560/abf717
35. Venerito V, Manfredi A, Lopalco G, Lavista M, Cassone G, Scardapane A, Sebastiani M, Iannone F. Radiomics to predict the mortality of patients with rheumatoid arthritis-associated interstitial lung disease: a proof-of-concept study. Front Med (Lausanne). 2022;9: 1069486.
36. Berenguer R, Pastor-Juan MDR, Canales-Vazquez J, Castro-Garcia M, Villas MV, Mansilla Legorburo F, Sabater S. Radiomics of CT features may be nonreproducible and redundant: influence of CT acquisition parameters. Radiology. 2018;288(2):407–15.
37. Xue C, Yuan J, Lo GG, Chang ATY, Poon DMC, Wong OL, Zhou Y, Chu WCW. Radiomics feature reliability assessed by intraclass correlation coefficient: a systematic review. Quant Imaging Med Surg. 2021;11(10):4431–60.

Publisher's Note